Molecular Crystals and Liquid Crystals

Publication details, including instructions for authors and subscription information:
http://www.tandfonline.com/loi/gmcl20

MOLECULAR AGGREGATION IN A HEMICYANINE DYE: MODELING BY A COMBINED CRYSTALLOGRAPHIC AND COMPUTATIONAL APPROACH

M. Sharath Chandra [a] & T. P. Radhakrishnan [a]

[a] School of Chemistry, University of Hyderabad, Hyderabad-500 046, India

Version of record first published: 02 Feb 2011

To cite this article: M. Sharath Chandra & T. P. Radhakrishnan (2003): MOLECULAR AGGREGATION IN A HEMICYANINE DYE: MODELING BY A COMBINED CRYSTALLOGRAPHIC AND COMPUTATIONAL APPROACH, Molecular Crystals and Liquid Crystals, 403:1, 77-103

To link to this article: http://dx.doi.org/10.1080/744818947

Mol. Cryst. Liq. Cryst., Vol. 403, pp. 77–103, 2003

ISSN: 1542-1406 print/1563-5287 online
DOI: 10.1080/15421400390233995

Taylor & Francis
Taylor & Francis Group

MOLECULAR AGGREGATION IN A HEMICYANINE DYE: MODELING BY A COMBINED CRYSTALLOGRAPHIC AND COMPUTATIONAL APPROACH

*M. Sharath Chandra and T. P. Radhakrishnan**
School of Chemistry, University of Hyderabad,
Hyderabad-500 046, India

Molecular aggregation in hemicyanine dye molecules, a problem of fundamental relevance to their linear and nonlinear optical properties, is addressed through a novel approach based on crystal structure investigation combined with semiempirical quantum chemical computations. Crystal structure of the hemicyanine salt N-n-butyl-4-[2-(4-dimethylaminophenyl) ethenyl] pyridinium bromide is investigated. The electronic absorption spectra of this compound in the solid state and in solution are modeled using semiempirical AM1/CI computations on the molecule and its dimers extracted from the crystal lattice; the molecular environment is mimicked by invoking a solvation model. This approach is shown to provide insight into the electronic absorption spectral shifts reported earlier for LB films of amphiphiles based on these chromophores and should prove useful in guiding further efforts at achieving deaggregation in these LB films.

Keywords: Hemicyanine dye; crystal structure; molecular aggregation; semiempirical computation

INTRODUCTION

Several polar dye molecules show a strong tendency to form aggregate structures in the fluid and ultrathin film states. The aggregate formation can significantly alter the linear and nonlinear optical characteristics of these compounds, often with adverse consequences. The electronic

Received 11 February 2003; accepted 6 May 2003.

Financial support from the Department of Science and Technology, New Delhi (Swarnajayanti Fellowship) and the use of the National Single Crystal Diffractometer Facility funded by the DST at the School of Chemistry, University of Hyderabad are acknowledged with gratitude. M. Sharath Chandra thanks the CSIR, New Delhi for a senior research fellowship.

*Corresponding author. E-mail: tprsc@uohyd.ernet.in

absorption peak shows significant wavelength shifts with respect to the monomer molecule as a result of exciton interactions in the aggregates [1]. Molecular aggregation usually leads to quenching of the fluorescence, though interesting exceptions are being reported [2]. Quadratic nonlinear optical phenomena such as second harmonic generation necessarily require a noncentric organization of the chromophores, and molecular aggregation of polar molecules often leads to centric structures pre-empting such applications [3]. Hemicyanines and merocyanines are important families of dye molecules [4], the aggregation of which has been studied extensively [5–9].

Aggregation of hemicyanine dye-based amphiphiles leads to the formation of H-aggregates in Langmuir-Blodgett (LB) films with consequent blue shift of the electronic absorption spectral peaks [6,7,10,11]. Earlier studies of this phenomenon have involved the investigation of electronic absorption [10,11], dynamics of emission [8], and second harmonic generation [3,6,9,12–14]. Investigations based on the extended dipole approximation have shown that, for the small intermolecular distances relevant to these systems, only H-aggregate behavior is manifested regardless of the axial orientation of molecules [11]. Extended dipole approximation has been employed also to analyze the spectral properties of stilbene aggregates in microheterogeneous media and monolayers [15]. The structures of these aggregates have been modeled through force field approaches utilizing cluster geometries from crystals [16].

We have demonstrated the impact of polyelectrolytes in the aqueous subphase on the stabilization of ionic amphiphiles spread at the air-water interface [17]. The polyelectrolyte methodology appears to be an efficient technique to effect deaggregation of hemicyanine based amphiphiles in monolayers. This would enable the fabrication of LB films of these chromophores for efficient optical second harmonic generation. In connection with these studies, we have considered the fundamental problem of aggregate formation of the hemicyanine headgroups. We have adopted a new approach involving the analysis of supramolecular clusters in molecular crystals of the hemicyanine dye as models for the aggregates and computation of their electronic structure through semiempirical quantum chemical methods. Similar studies that we have carried out on 4-nitroaniline–based systems have provided important insight into the correlation of molecular association in crystals and Langmuir/LB films [18]. Our approach is similar to that of Whitten and coworkers in the case of stilbenes [16], to the extent that we use supramolecular clusters from crystals to model the aggregate behavior; however, the utilization of semiempirical quantum chemical computations and the modeling of the spectroscopic features based on these clusters is a novel methodology. In this article, we present the crystal structure of the hemicyanine dye, N-*n*-butyl-4-[2-(4-dimethyl-

amino phenyl)ethenyl]pyridinium bromide (BDPB). A comparison of the electronic absorption spectra of the solution and microcrystalline solid clearly suggests the utility of the latter in modeling the electronic structure of molecular aggregates. We have carried out semiempirical computations incorporating solvation modeling which mimics the molecular environment not only in solution but also in the crystal lattice as shown in our earlier studies [19,20]. The calculations on the molecule and its clusters in the solid are used to model the electronic spectral features. These investigations provide a simple and convenient approach to visualizing aggregation of the hemicyanine dye molecule and suggest a structural basis to understand the spectroscopic features. This should prove useful in further studies on LB films and the fabrication of materials for photonic applications.

EXPERIMENTAL AND COMPUTATIONAL

Synthesis and Characterization

BDPB was synthesized following the procedure reported earlier [21]. First, 0.213 ml (2.193 mmol) of *n*-butylbromide was added to 0.235 ml (2.189 mmol) of 4-methylpyridine and stirred at 30°C for 36 h. Then 0.20 g (0.87 mmol) of N-butyl-4-methylpyridinium bromide obtained was mixed with 0.145 g (0.87 mmol) of 4-(N,N-dimethylamino)benzaldehyde and 0.10 ml of piperidine in methanol and refluxed for 2 h. On cooling the reaction mixture to 30°C, 0.17 g (54% yield) of BDPB precipitated out as a red crystalline solid. It was filtered, dried, and recrystallized several times from methanol. M. P./°C = 230 (dec.); FTIR (KBr): $\nu/cm^{-1} = 3016.9, 1641.6, 1575.9, 1157.4, 823.7$; UV-Vis (chloroform): $\lambda_{max}/nm = 497.5, 285.0$; ^{1}H-NMR ($CDCl_3$): δ/ppm = 0.95 (t, 3H), 1.41 (m, 2H), 1.95 (m, 2H), 3.06 (s, 6H), 4.66 (t, 2H), 6.65–6.70 (d, 2H), 6.80–6.89 (d, 1H), 7.50–7.54 (d, 2H), 7.57–7.65 (d, 1H), 7.84–7.88 (d, 2H), 8.94–8.97 (d, 2H); ^{13}C-NMR ($CDCl_3$): δ/ppm = 13.51, 19.39, 33.48, 40.07, 60.09, 112.00, 116.39, 122.38, 122.72, 130.67, 143.05, 143.46, 152.41, 154.20.

Electronic Absorption Spectroscopy

The electronic absorption spectrum of chloroform solution of BDPB was recorded on a Shimadzu Model UV-3101 UV-visible spectrometer. Samples for recording the spectrum of the solid material were prepared by dropping a solution/suspension of the material on a quartz plate, evaporating off the solvent and drying at 80°C. The specular reflectance (8° incidence) spectrum of the solid sample was recorded using the integrating sphere (ISR 3100) assembly of the spectrometer. The reflectance spectrum was converted into the absorption profile using the Kubelka-Munk function. We

have also investigated the electronic absorption of solid samples of BDPB ground with KBr and fabricated as a pellet. These samples gave spectra very similar to those of the solution indicating that the BDPB is molecularly dispersed in the solid solution and did not exhibit the signature of the molecular aggregates present in the crystalline solid.

Crystal Structure Determination

X-ray diffraction data were collected on an Enraf-Nonius MACH3 diffractometer. MoK_α radiation with a graphite crystal monochromator in the incident beam was used. Data was reduced using Xtal3.4 [22]; Lorentz and polarization corrections were included. Empirical absorption correction was applied using ψ-scan data. All nonhydrogen atoms were found using the direct method analysis in SHELX-97 [23], and after several cycles of refinement the positions of the hydrogen atoms were calculated and added to the refinement process. Graphics were handled using ORTEX6a [24]. Details of data collection, solution and refinement, fractional coordinates with anisotropic thermal parameters, and full lists of bond lengths and angles are submitted in the Appendix to this article.

Semiempirical Computations

Semiempirical quantum chemical studies were carried out using the AM1 [25] method in the MOPAC93 program package [26]. The microenvironment of the molecule in the crystal and the solution phase were simulated using the solvation model COSMO [27]; the parameter, (number of segments per atom) NSPA, was set equal to 60 in all calculations. The absorption energies were obtained from a configuration interaction (CI) calculation on geometries of the molecule and its supramolecular assemblies extracted from the crystal structure; H atom positions alone were optimized. The CI calculations invoked the full set of 400 singlet configurations involving 6 molecular orbitals bracketing the HOMO/LUMO.

RESULTS AND DISCUSSION

The electronic absorption spectrum of BDPB in chloroform solution and in the solid state are presented in Figure 1. The peak at 497.5 nm present in the solution spectrum is characteristic of the monomer [6–8,11]. Similar monomer peaks have been observed in LB films as well, where the hemicyanine dye has been deaggregated by admixing with fatty acids [6,8]. Spectra of BDPB recorded in solvents of different polarity clearly revealed the negative solvatochromism of this molecule, suggesting a strongly polar ground state. The absorption spectrum of the microcrystalline solid is

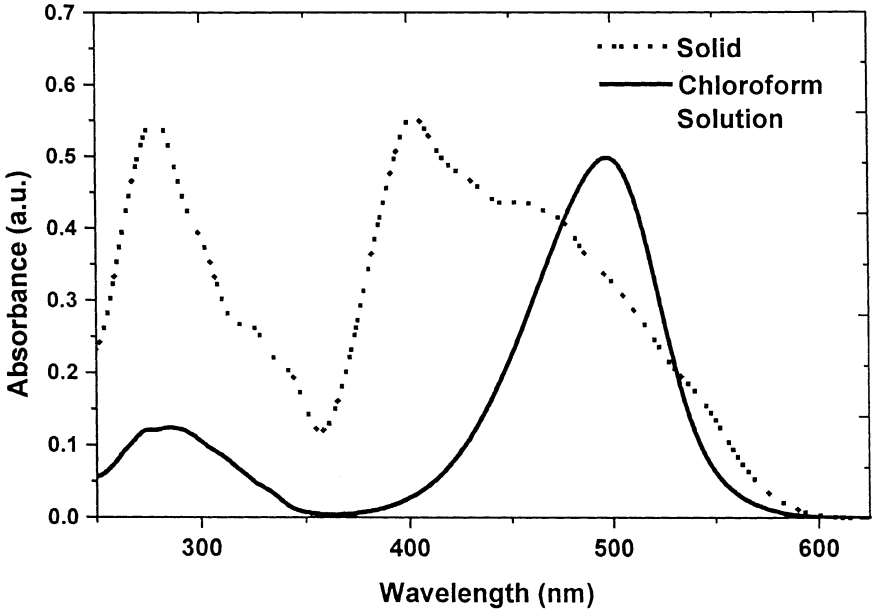

FIGURE 1 Electronic absorption spectra of BDPB in chloroform solution (full line) and in the solid state (broken line).

broad, and deconvolution indicates peaks at 460.2, 399.4, 327.2, and 278.7 nm. The new peaks at 399.4 and 327.2 nm appear to originate from the supramolecular aggregates present in the crystalline material. The absorption peaks near 340 nm in the spectra of Langmuir/LB films of amphiphiles based on similar chromophore as BDPB have been attributed [6,7,11] to molecular aggregates. To gain insight into the types of clusters that are relevant to model these spectral features, we have carried out single crystal X-ray diffraction analysis of BDPB.

Salts of N-methyl-4-[2-(4-dimethylaminophenyl)ethenyl]pyridinium have been reported to form predominantly noncentric crystal lattices [28]. X-ray analysis of crystals of BDPB grown by slow evaporation of methanolic solutions showed that they belong to the monoclinic $P2_1/c$ space group. The basic crystallographic data are collected in Table 1. The asymmetric unit consists of two molecules. The molecular structure is shown in Figure 2; since the structure of the two molecules in the asymmetric unit are very similar, only one is shown in the figure. It may be noted that the second bromide ion in the asymmetric unit resides close to the dimethylamino-phenyl group of the molecule shown in the figure. The aromatic region of the molecule is nearly planar with a very small twist of $\sim 4^\circ$ around the

TABLE 1 Crystallographic Data for BDPB

Molecular formula	$C_{19}H_{25}N_2Br$
Formula weight	361.32
Crystal system	Monoclinic
Space group	$P2_1/c$ (No.14)
a, Å	12.222 (10)
b, Å	17.521 (17)
c, Å	17.13 (2)
β, deg.	90.58 (9)
Z	8
$\rho_{calc.}$, g cm^{-3}	1.308
λ (Å)	0.71703
μ, cm^{-1}	22.50
Number of unique reflections	6433
Number of reflections with $I \geq 2\sigma_I$	3139
Number of parameters	397
GOF	1.002
T_{min} (empirical absorption correction)	0.7942
T_{max} (empirical absorption correction)	0.9995
R (for $I \geq 2\sigma_I$)	0.0621
wR^2	0.1336

central double bond. The butyl chain is all-*trans*. The significant bond lengths and angles are collected in Table 2. Figure 3 provides a view of the packing of molecules in the crystal of BDPB. The organic cation forms square channels running along the ***a*** axis with the bromide ions packed inside these channels. This packing motif appears to be facilitated by the strong Coulombic interactions likely to be present in this ionic solid. The crystal structure provides a basis to visualize possible molecular associations in different states of BDPB such as the solid, LB films, and solution. Below we analyze the electronic spectrum of BDPB in solution and in the solid state using semiempirical computations on the geometry of BDPB and its dimers extracted from the crystal structure. These computations also provide a model to understand the aggregate structures in LB films reported previously.

AM1/CI computations were carried out on the monomer of the cationic part of BDPB as well as the antiparallel and parallel dimer structures (Fig. 4) present in the crystal. Calculations employed different dielectric constants within the COSMO option. The computed λ_{max} and oscillator strength for the absorptions are collected in Table 3; those with oscillator strength < 0.25 are not shown. At all values of the dielectric constant, the lowest energy absorptions in both the dimers are found to be blue shifted with respect to the monomer. Based on a close examination of the computed absorption maxima and the peaks in the experimental spectra, the models

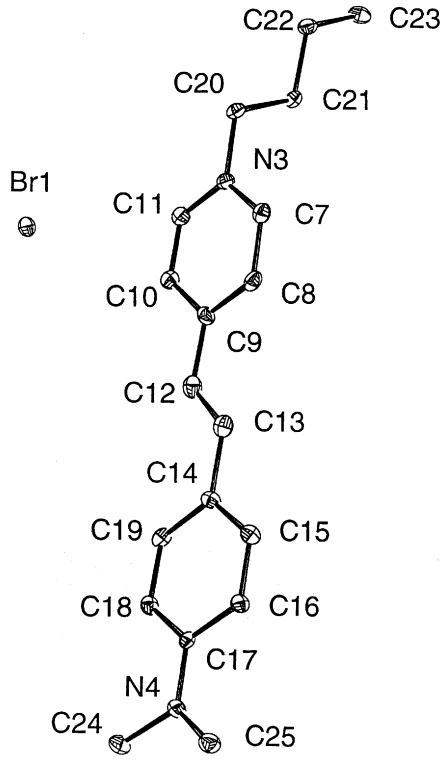

FIGURE 2 Molecular structure of BDPB from single crystal X-ray analysis; 10% probability thermal ellipsoids are indicated and H atoms are omitted for clarity. Structure of only one molecule in the asymmetric unit is shown.

that explain the experimental data are presented in Table 4. The agreement between the experimental values and the model calculations is quite good. The table also presents the data on LB films compiled from previous reports [6,9]; the data correspond to the hemicyanine dye based amphiphiles in pure form as well as composites with arachidic acid. Inspection of the experimental and computed data in Table 4 leads to the following conclusions. The monomer peaks are present in the solution, solid state, and LB film spectra. The antiparallel dimer explains the additional peaks in the solid state spectrum. Parallel dimer serves as a suitable model for the new peaks observed in the LB film spectrum. It should be noted that, even though the parallel dimer has the appearance of a traditional J-aggregate, the peaks are blue shifted. This result, obtained from a rigorous quantum chemical computation, is consistent with the experimental observation of only blue-shifted aggregate peaks in the LB films. It may be rationalized

TABLE 2 Significant Bond Lengths and Angles in BDPB

Bond	Length (Å)
N(3)-C(7)	1.347(8)
N(3)-C(11)	1.365(8)
N(3)-C(20)	1.475(7)
N(4)-C(17)	1.379(7)
N(4)-C(25)	1.449(8)
N(4)-C(24)	1.458(8)
C(7)-C(8)	1.386(9)
C(8)-C(9)	1.410(9)
C(9)-C(10)	1.380(9)
C(9)-C(12)	1.471(10)
C(10)-C(11)	1.339(9)
C(12)-C(13)	1.290(10)
C(13)-C(14)	1.490(9)
C(14)-C(15)	1.372(9)
C(14)-C(19)	1.391(9)
C(15)-C(16)	1.376(8)
C(16)-C(17)	1.399(8)
C(17)-C(18)	1.394(8)
C(18)-C(19)	1.389(9)
C(20)-C(21)	1.506(8)
C(21)-C(22)	1.526(8)
C(22)-C(23)	1.511(9)
Bond-bond	**Angle(°)**
C(7)-N(3)-C(11)	119.0(6)
C(7)-N(3)-C(20)	120.6(6)
C(11)-N(3)-C(20)	120.3(6)
C(17)-N(4)-C(25)	120.4(5)
C(17)-N(4)-C(24)	120.3(6)
C(25)-N(4)-C(24)	117.6(5)
N(3)-C(7)-C(8)	120.5(7)
C(7)-C(8)-C(9)	119.7(7)
C(10)-C(9)-C(8)	117.9(7)
C(10)-C(9)-C(12)	119.4(7)
C(8)-C(9)-C(12)	122.6(7)
C(11)-C(10)-C(9)	120.1(7)
C(10)-C(11)-N(3)	122.7(7)
C(13)-C(12)-C(9)	123.9(8)
C(12)-C(13)-C(14)	128.0(8)
C(15)-C(14)-C(19)	116.6(6)
C(15)-C(14)-C(13)	118.4(6)
C(19)-C(14)-C(13)	125.0(7)
C(14)-C(15)-C(16)	123.0(6)
C(15)-C(16)-C(17)	120.4(6)
N(4)-C(17)-C(18)	122.0(6)
N(4)-C(17)-C(16)	120.6(6)

(*Continued*)

TABLE 2 Continued

Bond—bond	Angle (°)
C(18)-C(17)-C(16)	117.3(6)
C(17)-C(18)-C(19)	120.7(6)
C(14)-C(19)-C(18)	121.7(6)
N(3)-C(20)-C(21)	113.1(5)
C(20)-C(21)-C(22)	111.0(5)
C(23)-C(22)-C(21)	111.9(5)

The values for only one of the molecules in the asymmetric unit are listed; see Figure 2 for atom labels.

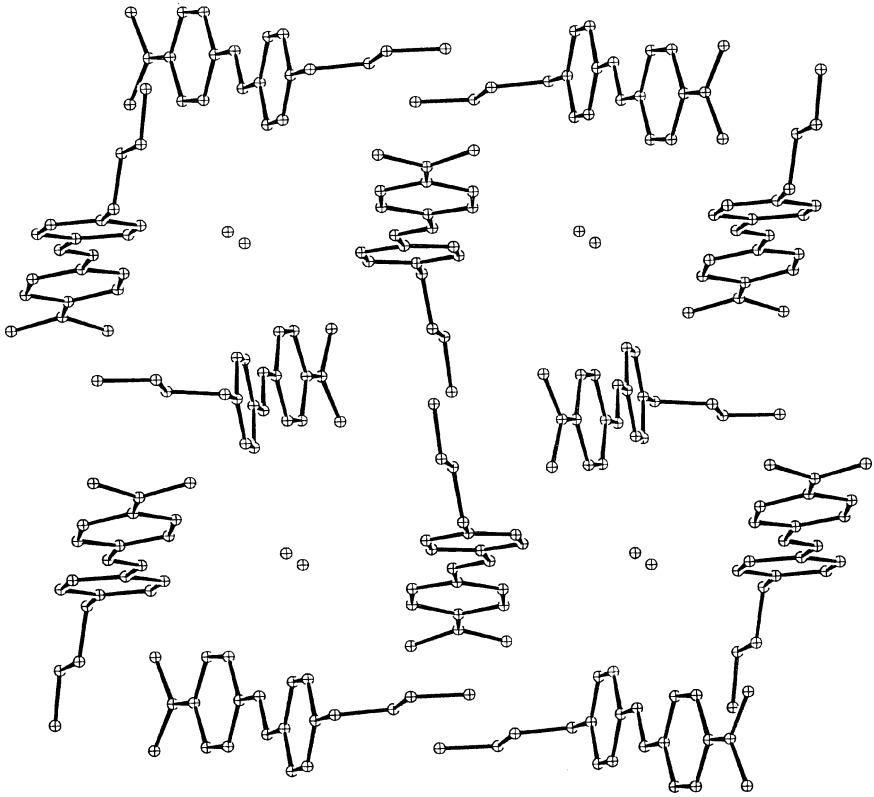

FIGURE 3 Packing of molecules in BDPB crystals viewed approximately along the a axis; H atoms are omitted for clarity. The spheres inside the channels are the bromide ions and the distance between the two ions shown within each cavity is 5.907 Å.

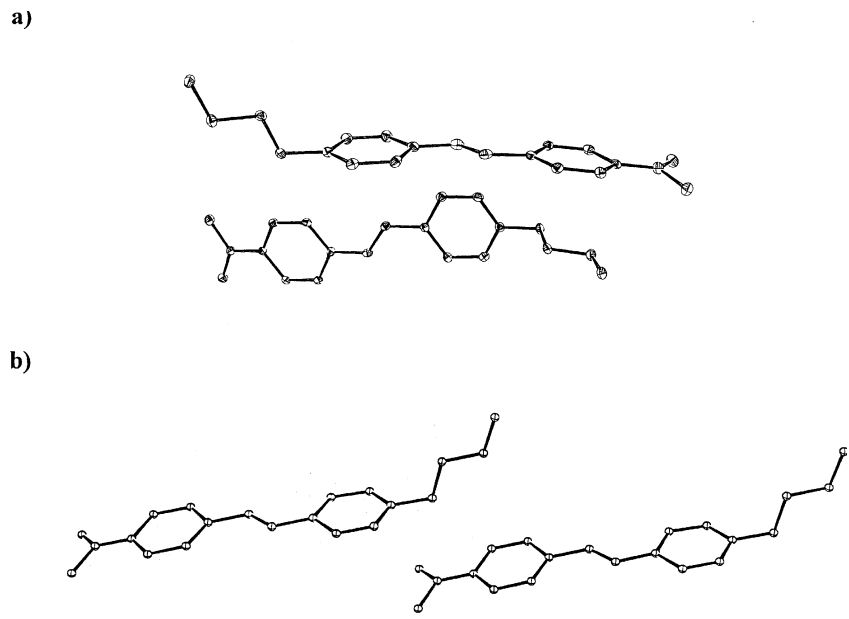

FIGURE 4 (a) Antiparallel and (b) parallel dimer structures of the cations present in BDPB crystals.

based on the fact that the simple point dipole approximation is not appropriate at short intermolecular distances where consideration of the extended dipole approximation predicts H-aggregate type behavior irrespective of molecular orientations [11]. It is seen that the molecular environment in the solution is modeled by a low dielectric constant close to

TABLE 3 Peak maximum (λ_{max}) and oscillator strength (f) for the electronic absorptions of monomer, antiparallel (Fig. 4a), and parallel (Fig. 4b) dimers of the cationic part of BDPB computed using the AM1/CI method under different dielectric constants ε in the COSMO routine

	λ_{max}(nm) [f]				
Structure	$\varepsilon = 1$	$\varepsilon = 2$	$\varepsilon = 3$	$\varepsilon = 4$	$\varepsilon = 5$
Monomer	506.6 [0.86]	476.4 [0.88]	450.2 [0.95]	435.8 [1.00]	426.9 [1.03]
	281.3 [0.32]	294.4 [0.57]	290.9 [0.61]	288.6 [0.60]	287.0 [0.54]
Dimer (antiparallel)	455.2 [0.90]	394.9 [0.87]	371.3 [0.88]	361.4 [0.90]	361.8 [0.96]
	393.6 [0.60]	344.7 [0.58]	325.7 [0.59]	315.9 [0.61]	310.0 [0.62]
Dimer (parallel)	466.5 [1.08]	403.3 [1.07]	379.2 [1.12]	369.1 [1.17]	368.0 [1.22]
	363.9 [0.76]	345.0 [0.75]	337.5 [0.73]	333.5 [0.72]	331.3 [0.72]

TABLE 4 Modeling of the electronic absorption peaks of BDPB in chloroform solution and in the solid state, and of similar chromophores in LB films, using selected computed λ_{max} from Table 3

	λ_{max} (nm)		
Sample	Experiment	AM1/CI calculation	Model
Solution (chloroform)	497.5	506.6	M (ε= 1)
	285.0	281.3	
LB Film	477.0,[a] 460.0[b]	476.4, 450.2[#]	M (ε= 2)
	339.0[a]	368.0,* 331.3*	[#]M (ε= 3)
	263.0[a]	294.4, 290.9[#]	*PD (ε= 5)
Solid	460.2	476.4	M (ε= 2)
	399.4	394.9*	*AD (ε= 2)
	327.2	344.7*	
	278.7	294.4	

[a]Scildkraut et al. [6]. The peaks at 339.0 and 263.0 nm are found in LB films of the pure dye and the peaks at 477.0 and 263.0 nm in LB films of the dye mixed with arachidic acid.

[b]Li et al. [9]. LB films of pure dye; the absorption in the UV region is not mentioned in this article.

M = monomer; AD = antiparallel dimer; PD = parallel dimer.

that of the solvent. The dielectric constant required to model the solid state is quite reasonable given the fact that the refractive index of organic crystals is typically 1.5–2.0 [20]. The molecular environment in the LB films is modeled using a low dielectric constant in the case of the hemicyanine dye mixed with the fatty acid, but by a relatively higher dielectric constant than that in the solution and solid states for the case of the pure dye; this is indicative of a more polarizable structure present in the LB films of the pure dye.

CONCLUSIONS

In the present study we have addressed the fundamental problem of dye molecule aggregation using detailed investigations of a hemicyanine molecule, a system of great interest in nonlinear optical applications. The crystal structure of a model compound was investigated to provide a basis for modeling aggregate structures. We employ a new approach based on semiempirical quantum chemical computations incorporating solvation modeling on molecular and supramolecular structures from the crystal to gain significant insight into the electronic absorption features of the solution and the solid state of the dye molecule. The current analysis leads also to a structural model to explain the monomer and aggregate absorption spectra of previously reported LB films of hemicyanine dye molecules.

The experimental and computational approach developed in the present study can be profitably used to monitor and model aggregation in LB films of new systems. Current work in progress in our laboratory will utilize the present analysis in the investigation of new approaches to achieve deaggregation of hemicyanine dye molecules in LB films. This will enable the development of techniques to enhance the optical second harmonic generation response of these ultrathin films.

REFERENCES

[1] Kasha, M., Rawls, H. R., & El-Bayoumi, M. A. (1965). *Pure Appl. Chem.*, *11*, 371–392.
[2] (a) Deans, R., Kim, J., Machacek, M. R., & Swager, T. M. (2000). *J. Am. Chem. Soc.*, *122*, 8565–8566.
(b) Levitus, M., Schmieder, K., Ricks, H., Shimizu, K. D., Bunz, U. H. F., & Garcia-Garibay, M. A. (2001). *J. Am. Chem. Soc.*, *123*, 4259–4265.
(c) Luo, J., Xie, Z., Lam, J. W. Y., Cheng, L., Chen, H., Qiu, C., Kwok, H. S., Zhan, X., Liu, Y., Zhu, D., & Tang, B. Z. (2001). *Chem. Commun.*, 1740–1741.
(d) An, B., Kwon, S., Jung, S., & Park, S. Y. (2002). *J. Am. Chem. Soc.*, *124*, 14410–14415.
[3] Carpenter, M. A., Willand, C. S., Penner, T. L., Williams, D. J., & Mukamel, S. (1992). *J. Phys. Chem.*, *96*, 2801–2804.
[4] Mishra, A., Behera, R. K., Behera, P. K., Mishra, B. K., & Behera, G. B. (2000). *Chem. Rev.*, *100*, 1973–2011.
[5] (a) Ashwell, G. J., Skjonnemand, K., Paxton, G. A. N., Allen, D. W., Mifflin, J. P. L., & Li, X. (2001). *J. Mater. Chem.*, *11*, 1351–1356.
(b) Würthner, G., Yao, S., Debaerdemaeker, T., & Wortmann, R. (2002). *J. Am. Chem. Soc.*, *124*, 9431–9447.
[6] Scildkraut, J. S., Penner, T. L., Willand, C. S., & Ulman, A. (1988). *Opt. Lett.*, *13*, 134–136.
[7] Evans, C. E., & Bohn, P. W. (1993). *J. Am. Chem. Soc.*, *115*, 3306–3311.
[8] Han, K., Lu, X., Xu, J., Zhou, G., Ma, S., Wang, W., Cai, Z., & Zhou, J. (1997). *J. Phys. D.*, *30*, 2923–2927.
[9] Li, F., Jin, L., Huang, C., Zheng, J., Guo, J., Zhao, X., & Liu, T. (2001). *Chem. Mater.*, *13*, 192–196.
[10] Alfimov, M. V., Lednev, I. K., & Styrkas, D. A. (1989). *Thin Solid Films*, *179*, 397–404.
[11] Evans, C. E., Song, Q., & Bohn, P. W. (1993). *J. Phys. Chem.*, *97*, 12302–12308.
[12] Hayden, L. M., Kowel, S. T., & Srinivasan, M. P. (1987). *Opt. Commun.*, *61*, 351–356.
[13] Marowsky, G., Chi, L. F., Möbius, D., Steinhoff, R., Shen, Y. R., Dorsch, D., & Rieger, B. (1988). *Chem. Phys. Lett.*, *147*, 420–424.
[14] (a) Kajikawa, K., Kigata, K., Takezoe, H., & Fukuda, A. (1990). *Mol. Cryst. Liq. Cryst.*, *182A*, 91–101.
(b) Ashwell, G. J. (1999). *J. Mater. Chem.*, *9*, 1991–2003.
[15] (a) Song, X., Geiger, C., Leinhos, U., Perlstein, J., & Whitten, D. G. (1994). *J. Am. Chem. Soc.*, *116*, 10340–10341.
(b) Song, X., Geiger, C., Farahat, M., Perlstein, J., & Whitten, D. G. (1997). *J. Am. Chem. Soc.*, *119*, 12481–12491.
[16] Vaday, S., Geiger, H. C., Cleary, B., Perlstein, J., & Whitten, D. G. (1997). *J. Phys. Chem.*, *101*, 321–329.

[17] Sharma, S., Sharath Chandra, M., & Radhakrishnan, T. P. (2001). *Langmuir*, *17*, 8118–8124.
[18] (a) Sharma, S., & Radhakrishnan, T. P. (2003). *J. Phys. Chem. B*, *107*, 147–156.
(b) Sharma, S., & Radhakrishnan, T. P. (2003). *Chem. Phys. Chem.*, *4*, 67–71.
[19] Sharma, S., & Radhakrishnan, T. P. (2000). *J. Phys. Chem. B*, *104*, 10191–10195.
[20] Jayanty, S., & Radhakrishnan, T. P. (2001). *Chem. Mater.*, *13*, 2460–2462.
[21] Girling, I. R., Cade, N. A., Kolinsky, P. V., Earls, J. D., Cross, G. H., & Peterson, I. R. (1985). *Thin Solid Films*, *132*, 101–112.
[22] Hall, S. R., King, G. S. D., & Stewart, J. M. (eds.). (1995). *Xtal3.4*, Crawley: University of Western Australia.
[23] Sheldrick, G. M. (1997). *SHELX-97*, Göttingen: University of Göttingen.
[24] McArdle, P. (1995). *J. Appl. Cryst.*, *28*, 65.
[25] Dewar, M. J. S., Zoebisch, E. G., Healy, E. F., & S Stewart, J. J. P. (1985). *J. Am. Chem. Soc.*, *107*, 3902–3907.
[26] *MOPAC93*, Tokyo: Fujitsu Inc.
[27] Klamt, A., & Shüürmann, G. (1993). *Perkin Trans. 2*, 799–805.
[28] Marder, S. R., Perry, J. W., & Yakymyshyn, C. P. (1994). *Chem. Mater.*, *6*, 1137–1147.

APPENDIX: SUPPLEMENTARY INFORMATION

Crystal Structure Determination

Single crystal X-ray data were measured on an ENRAF-NONIUS MACH3 diffractometer. MoK_α ($\lambda = 0.71073$ Å) radiation with a graphite crystal monochromator in the incident beam was used. The standard CAD4 centering, indexing, and data collection programs were used. The unit cell dimensions were obtained by a least-squares fit of 24 centered reflections near $\theta = 10°$. Intensity data were collected using the ω scan method at a scan speed of 4.12°/min. The scan width, $\Delta\theta$ for each reflection, was $[0.80 + 0.35\tan\theta]$. During data collection the intensities of three standard reflections were monitored every 1.5 h; no decay was observed. Three orientation standards were monitored every 250 reflections to monitor crystal motion. Data was reduced using Xtal3.4; intensities were corrected for Lorentz and polarization effects. Absorption correction was carried out using empirical psi-scan method. Non-H atoms were found using the SHELXS-97 direct method analysis and were refined anisotropically. H atoms were added at idealized positions for structure factor calculation, but were not refined (all computations were carried out on a Pentium PC using SHELXL-97). Refinement proceeded to convergence by minimizing $\Sigma w(F_o^2 - F_c^2)$. A final difference Fourier synthesis map showed the largest difference peak and hole to be very small. The R indices are calculated as $R = \Sigma|(|F_o| - |Fc|)|/\Sigma|F_o|$ and $wR^2 = [\Sigma w(F_o^2 - F_c^2)^2/\Sigma(F_o^2)^2]^{1/2}$. The crystallographic data are provided in the Tables A1 through A5, and the asymmetrical unit is shown in Fig. A1.

TABLE A1 Crystallographic Data for BDPB

Identification code	BDPB
Molecular formula	$C_{19}H_{25}N_2Br$
Formula weight	361.32
Crystal system	Monoclinic
Space group	$P2_1/c$ (No.14)
Color and appearance	Red grain
Dimensions, mm × mm × mm	0.64 × 0.48 × 0.32
a/Å	12.222(10)
b/Å	17.521(17)
c/Å	17.13(2)
β/deg.	90.58(9)
Z	8
μ, cm^{-1}	22.50
Temperature/K	293(2)
λ/Å	0.71703
θ range/deg.	1.66–24.97
No. of unique reflections	6433
No. of reflections with $I \geq 2\sigma_I$	3139
No. of parameters	397
GOF	1.002
$\rho_{calc.}$/g cm^{-3}	1.308
T_{min} (psi-scan absorption correction)	0.7942
T_{max}(psi-scan absorption correction)	0.9995
R [for $I \geq 2\sigma_I$]	0.0621
wR^2[for $I \geq 2\sigma_I$]	0.1336
R [all data]	0.1535
wR^2 [all data]	0.1763
Largest difference peak/e $Å^{-3}$	0.65
Largest difference hole/e $Å^{-3}$	−0.52

TABLE A2 Atomic Coordinates ($\times 10^4$) and Equivalent Isotropic Displacement Parameters ($Å \times 10^3$) for BDPB

	x	y	z	U_{eq}
Br(1)	9284(1)	2164(1)	2441(1)	62(1)
Br(2)	4453(1)	2166(1)	2504(1)	86(1)
N(3)	9377(4)	4904(3)	3008(3)	56(1)
N(4)	884(4)	4694(3)	1313(3)	59(2)
N(5)	5541(4)	2984(3)	−55(3)	53(1)
N(6)	14011(4)	1332(3)	−162(3)	53(1)

(*Continued*)

TABLE A2 Continued

	x	y	z	U_{eq}
C(7)	8694(6)	5497(4)	2891(4)	63(2)
C(8)	7595(6)	5373(4)	2728(4)	66(2)
C(9)	7191(6)	4620(5)	2682(4)	63(2)
C(10)	7925(6)	4029(4)	2782(4)	67(2)
C(11)	8976(6)	4179(4)	2951(4)	64(2)
C(12)	6043(7)	4446(5)	2486(4)	75(2)
C(13)	5302(7)	4960(5)	2372(4)	71(2)
C(14)	4139(6)	4846(4)	2128(4)	54(2)
C(15)	3492(6)	5478(4)	2026(4)	57(2)
C(16)	2429(5)	5440(3)	1757(4)	54(2)
C(17)	1952(5)	4735(4)	1577(3)	47(2)
C(18)	2581(6)	4084(4)	1710(4)	58(2)
C(19)	3652(6)	4142(4)	1982(4)	57(2)
C(20)	10540(5)	5034(4)	3205(4)	57(2)
C(21)	10739(5)	5166(4)	4064(3)	56(2)
C(22)	11926(5)	5394(4)	4223(4)	64(2)
C(23)	12162(6)	5482(4)	5086(4)	75(2)
C(24)	407(6)	3961(4)	1094(4)	75(2)
C(25)	310(6)	5377(4)	1066(4)	73(2)
C(26)	5975(6)	2862(4)	657(4)	60(2)
C(27)	7052(6)	2689(4)	751(4)	60(2)
C(28)	7752(5)	2639(3)	111(4)	48(2)
C(29)	7275(5)	2765(3)	−625(4)	51(2)
C(30)	6182(6)	2926(4)	−686(4)	55(2)
C(31)	8911(5)	2440(3)	217(4)	52(2)
C(32)	9642(5)	2384(3)	−352(4)	51(2)
C(33)	10770(5)	2148(3)	−273(4)	48(2)
C(34)	11281(5)	1981(3)	444(4)	51(2)
C(35)	12347(5)	1721(4)	480(4)	52(2)
C(36)	12960(5)	1594(3)	−199(4)	47(2)
C(37)	12443(5)	1785(4)	−917(3)	51(2)
C(38)	11390(5)	2046(4)	−938(3)	52(2)
C(39)	4380(5)	3207(4)	−164(4)	61(2)
C(40)	4248(5)	4065(4)	−232(4)	55(2)
C(41)	3078(5)	4273(4)	−446(4)	64(2)
C(42)	2892(5)	5131(4)	−460(4)	71(2)
C(43)	14480(5)	1056(4)	565(4)	68(2)
C(44)	14585(5)	1130(4)	−880(4)	64(2)

U_{eq} is defined as one third of the trace of the orthogonalized U_{ij} tensor.

TABLE A3 Bond Lengths [Å] and Angles [deg] for BDPB

Bond/bond	Distance/angle
N(3)-C(7)	1.347(8)
N(3)-C(11)	1.365(8)
N(3)-C(20)	1.475(7)
N(4)-C(17)	1.379(7)
N(4)-C(25)	1.449(8)
N(4)-C(24)	1.458(8)
N(5)-C(26)	1.342(8)
N(5)-C(30)	1.346(8)
N(5)-C(39)	1.482(7)
N(6)-C(36)	1.365(7)
N(6)-C(43)	1.449(8)
N(6)-C(44)	1.466(7)
C(7)-C(8)	1.386(9)
C(8)-C(9)	1.410(9)
C(9)-C(10)	1.380(9)
C(9)-C(12)	1.471(10)
C(10)-C(11)	1.339(9)
C(12)-C(13)	1.290(10)
C(13)-C(14)	1.490(9)
C(14)-C(15)	1.372(9)
C(14)-C(19)	1.391(9)
C(15)-C(16)	1.376(8)
C(16)-C(17)	1.399(8)
C(17)-C(18)	1.394(8)
C(18)-C(19)	1.389(9)
C(20)-C(21)	1.506(8)
C(21)-C(22)	1.526(8)
C(22)-C(23)	1.511(9)
C(26)-C(27)	1.359(9)
C(27)-C(28)	1.400(9)
C(28)-C(29)	1.401(8)
C(28)-C(31)	1.468(9)
C(29)-C(30)	1.368(8)
C(31)-C(32)	1.333(8)
C(32)-C(33)	1.444(8)
C(33)-C(38)	1.387(8)
C(33)-C(34)	1.403(8)
C(34)-C(35)	1.381(8)
C(35)-C(36)	1.407(8)
C(36)-C(37)	1.417(8)
C(37)-C(38)	1.366(8)
C(39)-C(40)	1.516(9)
C(40)-C(41)	1.517(8)
C(41)-C(42)	1.520(9)

(*Continued*)

TABLE A3 Continued

Bond/bond	Distance/angle
C(7)-N(3)-C(11)	119.0(6)
C(7)-N(3)-C(20)	120.6(6)
C(11)-N(3)-C(20)	120.3(6)
C(17)-N(4)-C(25)	120.4(5)
C(17)-N(4)-C(24)	120.3(6)
C(25)-N(4)-C(24)	117.6(5)
C(26)-N(5)-C(30)	119.4(6)
C(26)-N(5)-C(39)	121.7(6)
C(30)-N(5)-C(39)	118.9(6)
C(36)-N(6)-C(43)	121.0(5)
C(36)-N(6)-C(44)	120.1(5)
C(43)-N(6)-C(44)	116.9(5)
N(3)-C(7)-C(8)	120.5(7)
C(7)-C(8)-C(9)	119.7(7)
C(10)-C(9)-C(8)	117.9(7)
C(10)-C(9)-C(12)	119.4(7)
C(8)-C(9)-C(12)	122.6(7)
C(11)-C(10)-C(9)	120.1(7)
C(10)-C(11)-N(3)	122.7(7)
C(13)-C(12)-C(9)	123.9(8)
C(12)-C(13)-C(14)	128.0(8)
C(15)-C(14)-C(19)	116.6(6)
C(15)-C(14)-C(13)	118.4(6)
C(19)-C(14)-C(13)	125.0(7)
C(14)-C(15)-C(16)	123.0(6)
C(15)-C(16)-C(17)	120.4(6)
N(4)-C(17)-C(18)	122.0(6)
N(4)-C(17)-C(16)	120.6(6)
C(18)-C(17)-C(16)	117.3(6)
C(17)-C(18)-C(19)	120.7(6)
C(14)-C(19)-C(18)	121.7(6)
N(3)-C(20)-C(21)	113.1(5)
C(20)-C(21)-C(22)	111.0(5)
C(23)-C(22)-C(21)	111.9(5)
N(5)-C(26)-C(27)	121.2(6)
C(26)-C(27)-C(28)	121.3(6)
C(27)-C(28)-C(29)	116.3(6)
C(27)-C(28)-C(31)	121.0(6)
C(29)-C(28)-C(31)	122.7(6)
C(30)-C(29)-C(28)	119.9(6)
N(5)-C(30)-C(29)	121.9(6)
C(32)-C(31)-C(28)	125.5(6)
C(31)-C(32)-C(33)	126.8(6)
C(38)-C(33)-C(34)	116.8(6)
C(38)-C(33)-C(32)	119.2(6)

(*Continued*)

TABLE A3 Continued

Bond/bond	Distance/angle
C(34)-C(33)-C(32)	123.9(6)
C(35)-C(34)-C(33)	121.3(6)
C(34)-C(35)-C(36)	121.7(6)
N(6)-C(36)-C(35)	121.6(6)
N(6)-C(36)-C(37)	122.0(6)
C(35)-C(36)-C(37)	116.3(6)
C(38)-C(37)-C(36)	120.9(6)
C(37)-C(38)-C(33)	122.9(6)
N(5)-C(39)-C(40)	111.9(5)
C(39)-C(40)-C(41)	110.9(5)
C(40)-C(41)-C(42)	112.4(6)

TABLE A4 Anisotropic Displacement Parameters ($Å^2 \times 10^3$) for BDPB

	U_{11}	U_{22}	U_{33}	U_{23}	U_{13}	U_{12}
Br(1)	78(1)	58(1)	51(1)	0(1)	−2(1)	−2(1)
Br(2)	132(1)	62(1)	65(1)	−7(1)	−12(1)	32(1)
N(3)	47(4)	71(4)	49(3)	−1(3)	1(3)	1(3)
N(4)	57(4)	53(4)	67(4)	−6(3)	−5(3)	−7(3)
N(5)	49(4)	49(3)	61(4)	6(3)	3(3)	−1(3)
N(6)	43(3)	63(4)	54(3)	1(3)	4(3)	7(3)
C(7)	73(5)	59(5)	58(4)	−1(4)	1(4)	12(4)
C(8)	60(5)	85(6)	52(4)	−5(4)	−2(4)	30(4)
C(9)	69(5)	76(6)	42(4)	−10(4)	5(3)	−17(5)
C(10)	63(5)	68(5)	69(5)	−4(4)	2(4)	5(4)
C(11)	63(5)	69(5)	61(5)	−1(4)	1(4)	5(4)
C(12)	93(7)	67(5)	64(5)	0(4)	10(5)	−4(5)
C(13)	88(6)	76(6)	48(4)	8(4)	6(4)	6(5)
C(14)	51(5)	65(5)	45(4)	10(3)	0(3)	−11(4)
C(15)	62(5)	47(4)	62(4)	7(3)	−2(4)	−9(4)
C(16)	58(5)	39(4)	65(4)	3(3)	4(4)	−8(3)
C(17)	47(4)	53(4)	43(4)	−1(3)	9(3)	0(3)
C(18)	70(5)	44(4)	60(4)	−1(3)	8(4)	−12(4)
C(19)	62(5)	55(4)	53(4)	12(3)	6(4)	17(4)
C(20)	44(4)	72(5)	54(4)	3(4)	12(3)	4(3)
C(21)	53(4)	63(4)	52(4)	−1(3)	10(3)	6(3)
C(22)	46(4)	65(5)	80(5)	−2(4)	2(4)	3(4)
C(23)	60(5)	85(6)	79(5)	11(4)	−21(4)	−6(4)
C(24)	70(5)	71(5)	83(6)	−10(4)	−1(4)	−23(4)
C(25)	69(5)	74(5)	76(5)	0(4)	−14(4)	4(4)
C(26)	61(5)	68(5)	51(4)	2(4)	10(4)	4(4)
C(27)	62(5)	68(5)	51(4)	−5(4)	−1(4)	6(4)

(*Continued*)

TABLE A4 Continued

	U_{11}	U_{22}	U_{33}	U_{23}	U_{13}	U_{12}
C(28)	48(4)	38(4)	57(4)	−1(3)	−3(3)	−7(3)
C(29)	50(4)	52(4)	53(4)	−3(3)	5(3)	1(3)
C(30)	63(5)	54(4)	48(4)	2(3)	−7(4)	−1(4)
C(31)	60(4)	49(4)	48(4)	−3(3)	−8(3)	−3(3)
C(32)	62(5)	48(4)	44(4)	−1(3)	−1(3)	−2(3)
C(33)	43(4)	50(4)	49(4)	−1(3)	−4(3)	4(3)
C(34)	58(4)	47(4)	49(4)	6(3)	7(3)	2(3)
C(35)	56(4)	52(4)	48(4)	4(3)	−1(3)	7(3)
C(36)	46(4)	46(4)	48(4)	4(3)	2(3)	−1(3)
C(37)	49(4)	58(4)	44(4)	2(3)	9(3)	−3(3)
C(38)	50(4)	65(5)	42(4)	−2(3)	−1(3)	−3(3)
C(39)	41(4)	64(5)	79(5)	4(4)	0(4)	−5(4)
C(40)	46(4)	57(4)	64(4)	−1(3)	6(3)	−6(3)
C(41)	47(4)	82(6)	63(5)	−4(4)	−1(4)	6(4)
C(42)	50(4)	83(6)	81(5)	2(4)	7(4)	15(4)
C(43)	56(4)	78(5)	70(5)	−1(4)	3(4)	19(4)
C(44)	53(5)	80(5)	59(4)	1(4)	12(4)	13(4)

The anisotropic displacement factor exponent takes the form: $-2\,\pi^2\,[h^2\,a^{*2}U_{11}+\cdots+2\,h\,k\,a^*\,b^*\,U_{12}]$.

TABLE A5 Hydrogen coordinates ($\times 10^4$) and isotropic displacement parameters ($Å^2 \times 10^3$) for BDPB

	x	y	z	U_{eq}
H(7)	8961	5993	2920	76
H(8)	7125	5784	2650	79
H(10)	7690	3526	2733	80
H(11)	9452	3772	3032	77
H(12)	5839	3936	2443	90
H(13)	5520	5462	2451	85
H(15)	3785	5955	2145	68
H(16)	2024	5886	1694	65
H(18)	2281	3604	1615	70
H(19)	4055	3699	2068	68
H(20A)	10799	5474	2917	68
H(20B)	10963	4595	3040	68
H(21A)	10572	4704	4350	67
H(21B)	10257	5567	4246	67
H(22A)	12407	5008	4010	76
H(22B)	12078	5872	3961	76

(*Continued*)

TABLE A5 Continued

	x	y	z	U_{eq}
H(23A)	12910	5634	5162	112
H(23B)	12038	5004	5345	112
H(23C)	11688	5864	5299	112
H(24A)	−338	4034	927	112
H(24B)	426	3624	1536	112
H(24C)	818	3741	676	112
H(25A)	−421	5247	904	109
H(25B)	689	5607	638	109
H(25C)	282	5732	1493	109
H(26)	5531	2896	1093	72
H(27)	7330	2603	1251	72
H(29)	7701	2740	−1071	62
H(30)	5873	2998	−1179	66
H(31)	9156	2346	724	63
H(32)	9401	2509	−852	61
H(34)	10894	2047	904	62
H(35)	12669	1629	965	63
H(37)	12827	1733	−1380	61
H(38)	11074	2159	−1421	63
H(39A)	3960	3025	276	73
H(39B)	4091	2966	−632	73
H(40A)	4737	4258	−629	66
H(40B)	4446	4303	261	66
H(41A)	2588	4043	−72	77
H(41B)	2902	4065	−957	77
H(42A)	2142	5235	−594	107
H(42B)	3361	5360	−840	107
H(42C)	3056	5340	47	107
H(43A)	15219	892	479	102
H(43B)	14056	634	751	102
H(43C)	14477	1458	945	102
H(44A)	15309	955	−752	96
H(44B)	14630	1570	−1212	96
H(44C)	14191	732	−1147	96

SUMMARY OF SEMIEMPIRICAL AM1 CALCULATIONS

(These are provided in Tables A6 through A8)

TABLE A6 BDPB Cation Monomer

Final Geometry

							Charge
N	0.5603000	0	−3.7089000	0	0.3667000	0	−0.0609
N	0.1304000	0	6.9995000	0	−0.5288000	0	−0.2612
C	0.5851000	0	−3.0665000	0	1.5400000	0	−0.0044
H	0.7041783	1	−3.6853989	1	2.4577843	1	0.1970
C	0.4624000	0	−1.7121000	0	1.6128000	0	−0.1761
H	0.4917526	1	−1.2217052	1	2.6043601	1	0.1877
C	0.3040000	0	−0.9359000	0	0.4615000	0	0.1273
C	0.2850000	0	−1.6354000	0	−0.7499000	0	−0.1810
H	0.1687836	1	−1.1029834	1	−1.7103218	1	0.1837
C	0.4278000	0	−2.9977000	0	−0.7636000	0	−0.0095
H	0.4225380	1	−3.5632151	1	−1.7220907	1	0.1959
C	0.1898000	0	0.5215000	0	0.5524000	0	−0.2533
H	0.2710353	1	0.9152595	1	1.5812157	1	0.1508
C	0.0244000	0	1.3498000	0	−0.4863000	0	0.0602
H	−0.0769002	1	0.9314263	1	−1.5098113	1	0.1190
C	−0.0105000	0	2.7918000	0	−0.4454000	0	−0.1799
C	0.0612000	0	3.5393000	0	0.7423000	0	−0.0225
H	0.0832036	1	3.0276282	1	1.7173861	1	0.1324
C	0.0910000	0	4.9212000	0	0.7089000	0	−0.2292
H	0.1385666	1	5.4559546	1	1.6729337	1	0.1446
C	0.0915000	0	5.6371000	0	−0.5001000	0	0.1757
C	−0.0172000	0	4.8645000	0	−1.6858000	0	−0.2216
H	−0.0574445	1	5.3605946	1	−2.6695210	1	0.1469
C	−0.0511000	0	3.5031000	0	−1.6317000	0	−0.0317
H	−0.1182051	1	2.9474802	1	−2.5869318	1	0.1280
C	0.6204000	0	−5.1865000	0	0.2788000	0	−0.0564
H	1.1556619	1	−5.5666772	1	1.1954482	1	0.1319
H	1.2401966	1	−5.4504853	1	−0.6258760	1	0.1320
C	−0.7549000	0	−5.8101000	0	0.1793000	0	−0.1867
H	−1.3238205	1	−5.6443678	1	1.1335971	1	0.1048
H	−1.3468655	1	−5.3322828	1	−0.6476309	1	0.0999
C	−0.6559000	0	−7.3008000	0	−0.0888000	0	−0.1588
H	−0.0073168	1	−7.7778594	1	0.6932259	1	0.0894
H	−0.1599258	1	−7.4678392	1	−1.0814641	1	0.0883
C	−2.0137000	0	−7.9805000	0	−0.0891000	0	−0.2133
H	−1.8871379	1	−9.0690797	1	−0.3032837	1	0.0978
H	−2.6759494	1	−7.5372276	1	−0.8705744	1	0.0820
H	−2.5106213	1	−7.8681100	1	0.9040785	1	0.0830
C	0.3959000	0	7.7614000	0	0.6743000	0	−0.0824

(*Continued*)

TABLE A6 Continued

Final Geometry

							Charge
H	0.3826539	1	8.8582980	1	0.4432931	1	0.1029
H	1.3968676	1	7.4914790	1	1.1069794	1	0.0800
H	−0.4016595	1	7.5496154	1	1.4366906	1	0.0917
C	0.2697000	0	7.7044000	0	−1.8039000	0	−0.0821
H	0.3076019	1	8.8093215	1	−1.6237828	1	0.1031
H	−0.6168942	1	7.4733916	1	−2.4520128	1	0.0931
H	1.2076797	1	7.3848924	1	−2.3306396	1	0.0820

AM1 nointer precise XYZ charge = 1, 1SCF C.I. = 6, EPS = 1, NSPA = 60, GEO-OK MECI.
BDPB cation - Monomer from crystal structure-H atoms optimized.
Heat of formation = 206.811736 KCAL = 865.30030 KJ.
Electronic energy = −22142.932042 EV; State: singlet A.
Core-core repulsion = 18959.590408 EV.
Dipole = 7.10942 DEBYE; Symmetry: C1.
No. of filled levels = 54.
No. of open levels = 1.
Configuration interaction was used.
Charge on System = 1.
Ionization Potential = 12.659718 EV.
Homo (somo) lumo (EV) = −12.202 (−10.358) −4.791.
Molecular weight = 281.420.
SCF calculations = 2.

TABLE A7 BDPB Cation Dimer (Parallel)

Final Geometry

							Charge
N	6.7719000	0	5.2287000	0	−0.0942000	0	−0.0401
N	17.1273000	0	2.3326000	0	−0.2791000	0	−0.2951
C	7.2950000	0	5.0125000	0	1.1182000	0	0.0023
C	8.6133000	0	4.7122000	0	1.2814000	0	−0.1672
C	9.4761000	0	4.6183000	0	0.1862000	0	0.1181
C	8.8997000	0	4.8462000	0	−1.0680000	0	−0.1726
C	7.5637000	0	5.1302000	0	−1.1732000	0	−0.0039
C	10.8883000	0	4.2780000	0	0.3743000	0	−0.2247
C	11.7953000	0	4.1751000	0	−0.6051000	0	0.0274
C	13.1717000	0	3.7641000	0	−0.4692000	0	−0.1582
C	13.7792000	0	3.4710000	0	0.7635000	0	−0.0306
C	15.0838000	0	3.0165000	0	0.8202000	0	−0.2352
C	15.8444000	0	2.7897000	0	−0.3390000	0	0.1417
C	15.2244000	0	3.1258000	0	−1.5709000	0	−0.2295
C	13.9392000	0	3.5778000	0	−1.6055000	0	−0.0388
C	5.3570000	0	5.6266000	0	−0.2798000	0	−0.0611
C	5.1953000	0	7.1266000	0	−0.3974000	0	−0.1862
C	3.7680000	0	7.4907000	0	−0.7642000	0	−0.1591

(*Continued*)

TABLE A7 Continued

Final Geometry

							Charge
C	3.5410000	0	8.9919000	0	−0.7868000	0	−0.2138
C	17.6877000	0	1.8508000	0	0.9669000	0	−0.0807
C	17.8393000	0	1.9769000	0	−1.5074000	0	−0.0803
H	6.6094101	1	5.0878641	1	1.9916340	1	0.2048
H	9.0012451	1	4.5374261	1	2.3038944	1	0.1901
H	9.5034716	1	4.7868695	1	−1.9910578	1	0.1843
H	7.0923632	1	5.3037851	1	−2.1673839	1	0.2032
H	11.1644366	1	4.0786953	1	1.4255112	1	0.1507
H	11.4980384	1	4.3943084	1	−1.6522129	1	0.1249
H	13.2173063	1	3.6005202	1	1.7025106	1	0.1403
H	15.5008075	1	2.7867706	1	1.8153826	1	0.1434
H	15.7638148	1	2.9827393	1	−2.5217571	1	0.1450
H	13.4932628	1	3.7982103	1	−2.5950471	1	0.1368
H	4.7702385	1	5.2392783	1	0.6015917	1	0.1375
H	4.9752681	1	5.1121358	1	−1.2091426	1	0.1378
H	5.4632915	1	7.6223018	1	0.5741888	1	0.1054
H	5.8853813	1	7.5377540	1	−1.1828626	1	0.0983
H	3.0635728	1	7.0253163	1	−0.0245339	1	0.0924
H	3.5228744	1	7.0652346	1	−1.7732062	1	0.0906
H	2.4802061	1	9.2044248	1	−1.0638295	1	0.1029
H	4.2097924	1	9.4803546	1	−1.5350708	1	0.0817
H	3.7433655	1	9.4371789	1	0.2165516	1	0.0838
H	18.7315009	1	1.4754318	1	0.8014486	1	0.1012
H	17.0688311	1	1.0145692	1	1.3943132	1	0.0983
H	17.7197654	1	2.6939354	1	1.7097256	1	0.0673
H	18.8487288	1	1.5595583	1	−1.2588305	1	0.1020
H	17.9685620	1	2.8996639	1	−2.1334517	1	0.0664
H	17.2644106	1	1.2109214	1	−2.0946575	1	0.1004
N	18.9941000	0	5.2287000	0	−0.0942000	0	−0.0565
N	29.3495000	0	2.3326000	0	−0.2791000	0	−0.2564
C	19.5172000	0	5.0125000	0	1.1182000	0	−0.0058
C	20.8355000	0	4.7122000	0	1.2814000	0	−0.1797
C	21.6983000	0	4.6183000	0	0.1862000	0	0.1320
C	21.1219000	0	4.8462000	0	−1.0680000	0	−0.1841
C	19.7859000	0	5.1302000	0	−1.1732000	0	−0.0117
C	23.1105000	0	4.2780000	0	0.3743000	0	−0.2674
C	24.0175000	0	4.1751000	0	−0.6051000	0	0.0710
C	25.3939000	0	3.7641000	0	−0.4692000	0	−0.1904
C	26.0014000	0	3.4710000	0	0.7635000	0	−0.0192
C	27.3060000	0	3.0165000	0	0.8202000	0	−0.2310
C	28.0666000	0	2.7897000	0	−0.3390000	0	0.1799
C	27.4466000	0	3.1258000	0	−1.5709000	0	−0.2227
C	26.1614000	0	3.5778000	0	−1.6055000	0	−0.0296
C	17.5792000	0	5.6266000	0	−0.2798000	0	−0.0539
C	17.4175000	0	7.1266000	0	−0.3974000	0	−0.1865

(*Continued*)

TABLE A7 Continued

Final Geometry

							Charge
C	15.9902000	0	7.4907000	0	−0.7642000	0	−0.1560
C	15.7632000	0	8.9919000	0	−0.7868000	0	−0.2142
C	29.9099000	0	1.8508000	0	0.9669000	0	−0.0855
C	30.0615000	0	1.9769000	0	−1.5074000	0	−0.0851
H	18.8326086	1	5.0951894	1	1.9911308	1	0.1920
H	21.2292331	1	4.5460151	1	2.3027859	1	0.1882
H	21.7295805	1	4.7941435	1	−1.9885932	1	0.1844
H	19.3163547	1	5.3093376	1	−2.1653664	1	0.1917
H	23.3922364	1	4.0893210	1	1.4257019	1	0.1521
H	23.7210631	1	4.3956051	1	−1.6521308	1	0.1182
H	25.4442546	1	3.6142864	1	1.7028683	1	0.1322
H	27.7374535	1	2.8166962	1	1.8160232	1	0.1473
H	27.9974719	1	3.0092728	1	−2.5189408	1	0.1498
H	25.7201076	1	3.8097842	1	−2.5939203	1	0.1281
H	16.9914152	1	5.2327897	1	0.5984403	1	0.1302
H	17.1958299	1	5.1083944	1	−1.2072709	1	0.1304
H	17.6869163	1	7.6217210	1	0.5742134	1	0.1064
H	18.1092804	1	7.5392301	1	−1.1814485	1	0.1028
H	15.2876460	1	7.0245418	1	−0.0240257	1	0.0826
H	15.7458129	1	7.0664482	1	−1.7726676	1	0.0837
H	14.7035492	1	9.2075934	1	−1.0633273	1	0.0898
H	16.4332169	1	9.4798851	1	−1.5348112	1	0.0874
H	15.9681202	1	9.4366924	1	0.2158788	1	0.0856
H	30.9447466	1	1.4555366	1	0.7966474	1	0.1072
H	29.2744982	1	1.0322938	1	1.4015011	1	0.0816
H	29.9678437	1	2.6979910	1	1.7026479	1	0.0935
H	31.0800244	1	1.5843932	1	−1.2560879	1	0.1072
H	30.1759427	1	2.8930843	1	−2.1453346	1	0.0952
H	29.4950916	1	1.1943332	1	−2.0786979	1	0.0835

AM1 nointer precise XYZ charge = +2, C.I. = 6, MECI NSPA = 60, GEO-OK EPS = 1, 1SCF.
BDPB cation-parallel dimer from crystal structure-H atoms optimized.
Heat of formation = 445.282950 KCAL = 1863.06386 KJ.
Electronic energy = −61922.732381 EV; State: Singlet A.
Core-core repulsion = 55557.421998 EV.
Dipole = 17.43536 DEBYE; Symmetry: C1.
No. of filled levels = 109.
No. of open levels = 1.
Configuration interaction was used.
Charge on system = 2.
Ionization potential = 14.757365 EV.
Homo (somo) lumo (EV) = −12.452 (−11.263) −6.254.
Molecular weight = 562.840.
SCF calculations = 2.

TABLE A8 BDPB Cation Dimer (Antiparallel)

Final Geometry

							Charge
N	2.3179000	0	0.1033000	0	−3.6322000	0	−0.0530
N	−8.0325000	0	−1.3008000	0	−1.0625000	0	−0.2773
N	−2.3179000	0	−0.2560000	0	2.5922000	0	−0.0560
N	8.0376000	0	1.9785000	0	4.4439000	0	−0.2541
C	1.4855000	0	−0.8492000	0	−4.0811000	0	0.0171
H	1.9048445	1	−1.6340502	1	−4.7487800	1	0.2103
C	0.1490000	0	−0.8392000	0	−3.7261000	0	−0.1761
H	−0.5106553	1	−1.6307106	1	−4.1196404	1	0.1924
C	−0.3435000	0	0.1774000	0	−2.8857000	0	0.1157
C	0.5498000	0	1.1216000	0	−2.4167000	0	−0.1687
H	0.2064560	1	1.9336113	1	−1.7475771	1	0.1820
C	1.8293000	0	1.0762000	0	−2.8058000	0	−0.0020
H	2.5710894	1	1.8399741	1	−2.4748390	1	0.1969
C	−1.7406000	0	0.2344000	0	−2.4318000	0	−0.2382
H	−1.9584755	1	1.0721943	1	−1.7435099	1	0.1382
C	−2.6487000	0	−0.6093000	0	−2.8012000	0	0.0367
H	−2.4186140	1	−1.4158363	1	−3.5314812	1	0.1287
C	−4.0692000	0	−0.6972000	0	−2.3487000	0	−0.1688
C	−4.8590000	0	−1.6926000	0	−2.8575000	0	−0.0456
H	−4.4522244	1	−2.3684868	1	−3.6354149	1	0.1340
C	−6.1542000	0	−1.9116000	0	−2.4469000	0	−0.2094
H	−6.7187951	1	−2.7379725	1	−2.9110333	1	0.1587
C	−6.7292000	0	−1.0968000	0	−1.4701000	0	0.1648
C	−5.9695000	0	−0.0386000	0	−0.9872000	0	−0.2274
H	−6.3854591	1	0.6820561	1	−0.2646530	1	0.1433
C	−4.6638000	0	0.1535000	0	−1.4251000	0	−0.0590
H	−4.0969548	1	1.0109801	1	−1.0258057	1	0.1106
C	3.7385000	0	0.1221000	0	−4.0363000	0	−0.0593
H	4.0897041	1	−0.9506168	1	−4.0827125	1	0.1358
H	4.3240373	1	0.6458418	1	−3.2266562	1	0.1321
C	3.9644000	0	0.7995000	0	−5.3665000	0	−0.1900
H	3.7238103	1	1.8938591	1	−5.2924131	1	0.1060
H	3.2920713	1	0.3629233	1	−6.1537212	1	0.1039
C	5.4121000	0	0.6392000	0	−5.8226000	0	−0.1545
H	6.0966881	1	1.0222897	1	−5.0202154	1	0.0884
H	5.6360124	1	−0.4515830	1	−5.9618368	1	0.0908
C	5.6849000	0	1.3780000	0	−7.1101000	0	−0.2162
H	6.7480683	1	1.2210453	1	−7.4164812	1	0.1041
H	5.5108604	1	2.4738565	1	−6.9839853	1	0.0845
H	5.0228746	1	1.0072351	1	−7.9292017	1	0.0856
C	−8.6111000	0	−0.4807000	0	−0.0074000	0	−0.0788
H	−9.6638448	1	−0.8066744	1	0.1951151	1	0.1120
H	−8.6240024	1	0.5928558	1	−0.3351414	1	0.0943
H	−8.0122651	1	−0.5692755	1	0.9387513	1	0.0621
C	−8.7296000	0	−2.5149000	0	−1.4208000	0	−0.0824

(*Continued*)

TABLE A8 Continued

Final Geometry

							Charge
H	−9.7570358	1	−2.5169233	1	−0.9708058	1	0.1090
H	−8.1695423	1	−3.4184911	1	−1.0558872	1	0.0741
H	−8.8358995	1	−2.5759787	1	−2.5378964	1	0.0965
C	−1.7949000	0	0.6315000	0	1.7384000	0	−0.0025
H	−2.4859019	1	1.0791223	1	0.9901199	1	0.1885
C	−0.4766000	0	0.9705000	0	1.7828000	0	−0.1903
H	−0.0918995	1	1.7273664	1	1.0765317	1	0.1700
C	0.3863000	0	0.4028000	0	2.7241000	0	0.1322
C	−0.1901000	0	−0.5188000	0	3.6048000	0	−0.1794
H	0.4134562	1	−1.0072768	1	4.3904272	1	0.1888
C	−1.5260000	0	−0.8104000	0	3.5230000	0	−0.0004
H	−1.9973661	1	−1.5321940	1	4.2281608	1	0.2027
C	1.7985000	0	0.7886000	0	2.7719000	0	−0.2751
H	2.0720535	1	1.5755081	1	2.0477096	1	0.1397
C	2.7055000	0	0.2962000	0	3.6247000	0	0.0733
H	2.4087328	1	−0.4989968	1	4.3413243	1	0.1243
C	4.0820000	0	0.7086000	0	3.7564000	0	−0.1938
C	4.6893000	0	1.6703000	0	2.9313000	0	−0.0252
H	4.1282176	1	2.1145464	1	2.0951584	1	0.1209
C	5.9939000	0	2.0713000	0	3.1525000	0	−0.2342
H	6.4224904	1	2.8256932	1	2.4712076	1	0.1433
C	6.7546000	0	1.5734000	0	4.2237000	0	0.1818
C	6.1347000	0	0.5775000	0	5.0229000	0	−0.2199
H	6.6838947	1	0.1183971	1	5.8621907	1	0.1544
C	4.8495000	0	0.1914000	0	4.7852000	0	−0.0260
H	4.4066189	1	−0.5741590	1	5.4515658	1	0.1330
C	−3.7328000	0	−0.6869000	0	2.5084000	0	−0.0567
H	−4.3217990	1	0.1440505	1	2.0255220	1	0.1305
H	−4.1122889	1	−0.8196706	1	3.5629271	1	0.1381
C	−3.8945000	0	−1.9697000	0	1.7220000	0	−0.1860
H	−3.6292730	1	−1.7958747	1	0.6440727	1	0.1023
H	−3.2034201	1	−2.7641133	1	2.1145004	1	0.0999
C	−5.3217000	0	−2.4798000	0	1.8048000	0	−0.1578
H	−6.0242293	1	−1.6670528	1	1.4744531	1	0.0866
H	−5.5685270	1	−2.7264996	1	2.8712342	1	0.0936
C	−5.5487000	0	−3.7077000	0	0.9408000	0	−0.2144
H	−6.6017647	1	−4.0593612	1	1.0590308	1	0.0967
H	−4.8612558	1	−4.5343305	1	1.2397187	1	0.0853
H	−5.3761888	1	−3.4674517	1	−0.1358282	1	0.0798
C	8.5979000	0	3.1006000	0	3.7190000	0	−0.0860
H	9.6414087	1	3.3055826	1	4.0741627	1	0.1109
H	7.9754336	1	4.0236889	1	3.8664851	1	0.0840
H	8.6374612	1	2.8566703	1	2.6232513	1	0.0880
C	8.7496000	0	1.5444000	0	5.6467000	0	−0.0872
H	9.7675534	1	2.0113703	1	5.6750455	1	0.1100

(*Continued*)

TABLE A8 Continued

Final Geometry

							Charge
H	8.8653907	1	0.4283551	1	5.6230853	1	0.0960
H	8.1821853	1	1.8406665	1	6.5692540	1	0.0886

AM1 nointer precise XYZ charge = +2, C.I. = 6, MECI EPS = 1, NSPA = 60, GEO-OK 1SCF.
BDPB cation-antiparallel dimer from crystal structure-H atoms optimized.
Heat of formation = 461.321310 KCAL = 1930.16836 KJ.
Electronic energy = −65246.470299 EV; State: Singlet A.
Core-core repulsion = 58881.855405 EV.
Dipole = 3.40179 DEBYE; Symmetry: C1.
No. of filled levels = 109.
No. of open levels = 1.
Configuration interaction was used.
Charge on System = 2.
Ionization Potential = 15.374944 EV.
Homo (somo) lumo (EV) = −12.230 (−11.855) −6.737.
Molecular weight = 562.840.
SCF calculations = 2.

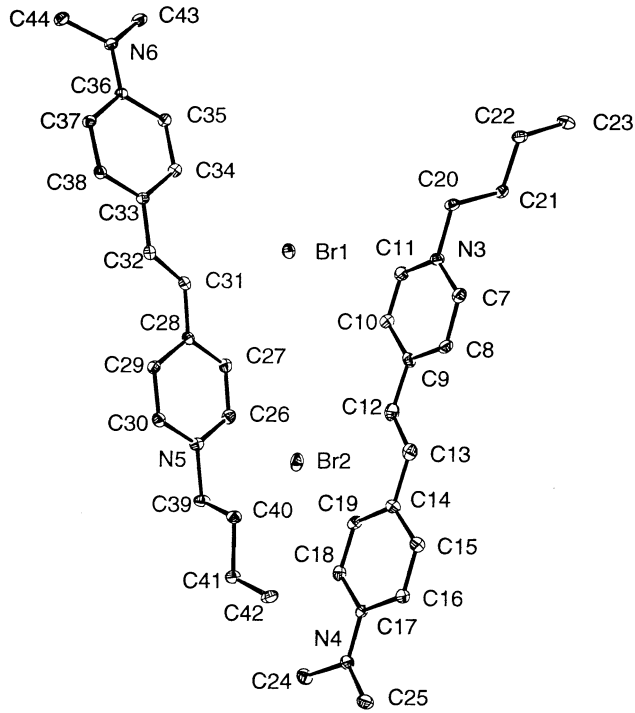

FIGURE A1 Molecular structure of the asymmetric unit in BDPB